Supporting Information

Air-Stable Room-Temperature Mid-Infrared Photodetectors Based on hBN/Black Arsenic Phosphorus/hBN Heterostructures

Shaofan Yuan[†,Δ], Chenfei Shen[‡, Δ], Bingchen Deng[†], Xiaolong Chen[†], Qiushi Guo[†], Yuqiang Ma[¤], Ahmad Abbass[¤,1,2,3], Bilu Liu[¤,4], Ralf Haiges[w], Claudia Ott[§], Tom Nilges[§], Kenji Watanabe[‖], Takashi Taniguchi[‖], Ofer Sinai[⊥], Doron Naveh[⊥], Chongwu Zhou*[‡,¤] and Fengnian Xia*[†]

[†]Department of Electrical Engineering, Yale University, New Haven, Connecticut 06511, United States

[‡] Mork Family Department of Chemical Engineering and Materials Science, University of Southern California, Los Angeles, California 90089, United States

[¤] Ming Hsieh Department of Electrical Engineering, University of Southern California, Los Angeles, California 90089, United States

[w] Loker Hydrocarbon Research Institute and Department of Chemistry, University of Southern California, Los Angeles, California 90089, United States

[§] Department of Chemistry, Technical University Munich, Lichtenbergstr.4, 85748 Garching b. München, Germany

[‖]National Institute for Materials Science, 1-1 Namiki, Tsukuba, 305-0044, Japan

$\perp$Faculty of Engineering and Bar-Ilan Institute for Nanotechnology and Advanced Materials,

Bar-Ilan University, Ramat-Gan 52900, Israel

Corresponding Author

* E-mail: fengnian.xia@yale.edu and chongwuz@usc.edu

I. The elemental composition analysis of b-As$_{0.83}$P$_{0.17}$.

Element	Wt %	At %
As	92.19	82.98
P	07.81	17.02

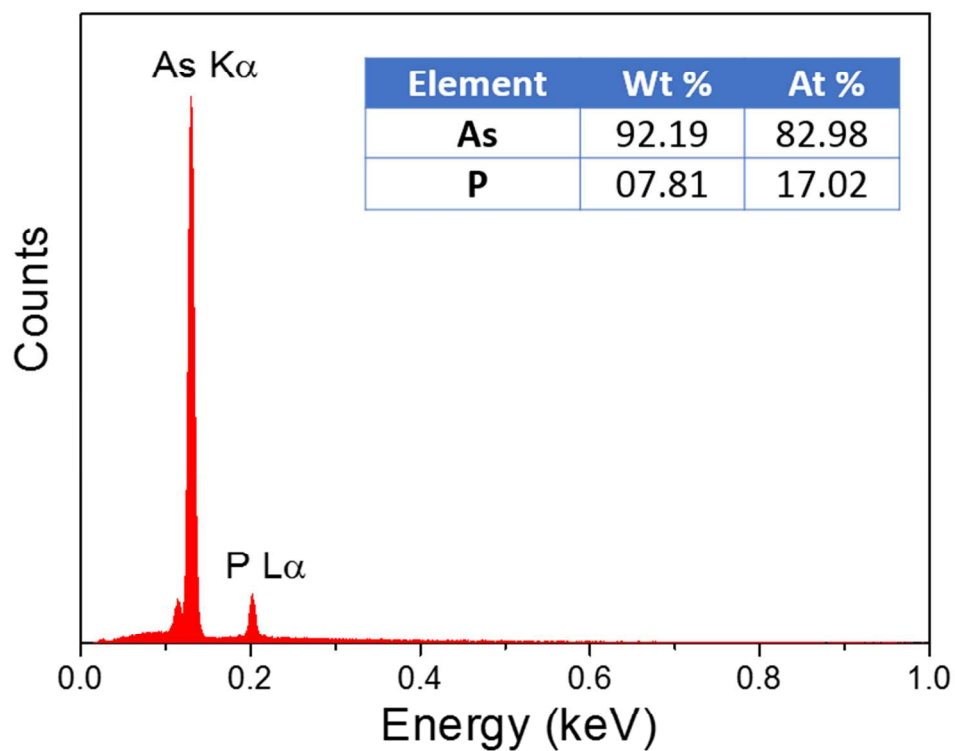**Figure S1.** EDS spectrum of As$_{0.83}$P$_{0.17}$. The elemental composition is summarized in the inset table. The relative abundance is calculated considering the X-ray emission peaks of As Kα and P Lα transitions.[1]

II. The crystallographic information of b-$As_{0.83}P_{0.17}$.

Empirical formula	$As_{0.83}P_{0.17}$
Space group	Cmca
Crystal system	orthorhombic
Unit cell dimensions	a=3.561(3) Å $\quad$ α=90°
	b=10.803(9) Å $\quad$ β=90°
	c=4.493(4) Å $\quad$ γ=90°
Volume	172.8(3) Å^3
Z	8
Calculated density	5.759 g/cm^3
Transmission ratio (max/min)	0.3950/0.1310
Absorption coefficient	38.049 mm^{-1}
F(000)	264
θ range	3.77°-30.30°
Total number of reflections	763
Independent reflections	147 (R_{int} = 0.0467)
Data/restraints/parameters	147/0/7
Goodness-of-fit on F^2	1.101
Final R indices [I > 2σ(I)]	R_1 = 0.0334
	wR_2 = 0.0760
R indices (all data)	R_1 = 0.0364
	wR_2 = 0.0775
Largest diff. peak and hole	1.239 and -2.215 eÅ^{-3}

Table S1. Summary of crystallographic data of the b-$As_{0.83}P_{0.17}$ measured at 100 K.

In the refinement, standard parameters are used in the SHELXTL software as explained below.[2,3] $F_o(hkl)$ and $F_c(hkl)$ are the observed and calculated structure factor corresponding to certain Miller index (hkl). The diffraction intensity I_{hkl} is related to F(hkl) by $I_{hkl} \propto |F(hkl)|^2$, and σ is the standard uncertainty. The merging residuals from merging equivalent reflections, such as Friedel opposites, are defined as $R_{int} = \frac{\sum|F_o^2-\langle F_o^2\rangle|}{\sum F_o^2}$ and $R_{sig} = \frac{\sum \sigma(F_o^2)}{\sum F_o^2}$. The residual factors of the

structure refinement are defined as $R_1 = \frac{\sum||F_o|-|F_c||}{\sum|F_o|}$ and $wR_2 = \sqrt{\frac{\sum w(F_o^2-F_c^2)^2}{\sum wF_o^2}}$, where w is the weight parameter and F_o and F_c are the observed and calculated structure factors. The Goodness-of-fit S is

defined by $S = \sqrt{\frac{\sum w(F_o^2 - F_c^2)^2}{(N_R - N_P)}}$, where N_R is the number of independent reflections and N_P is the

number of refined parameters.
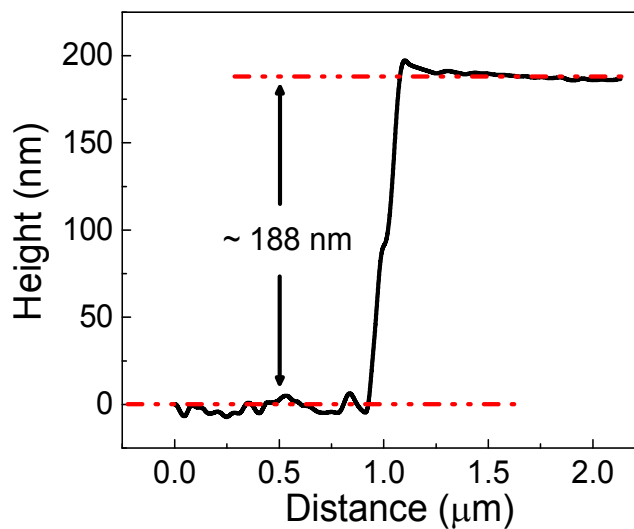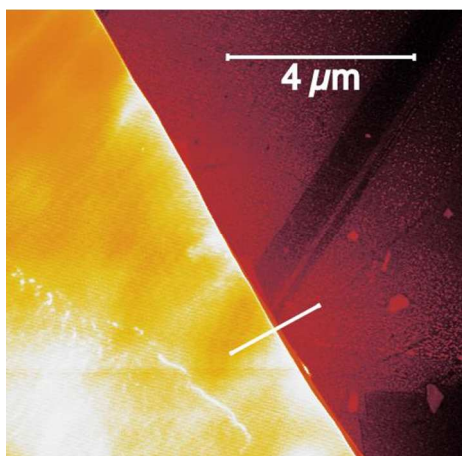
III. The thickness profile of the exfoliated b-As$_{0.83}$P$_{0.17}$ shown in Figure 1c.

Figure S2. The thickness profile of the exfoliated b-As$_{0.83}$P$_{0.17}$ flake used for extinction spectra characterization acquired using atomic force microscope.

IV. The reflection measurements of b-As$_{0.83}$P$_{0.17}$ flake on ZnS substrate

The reflection measurements were performed on the same flake as shown in Figure 1c. The optical configuration for extinction and reflection measurements are drawn in Figure S4 a and b. In the reflection spectra below, R is the reflection of b-As$_{0.83}$P$_{0.17}$ flake on ZnS substrate, and R$_0$ corresponds to the reflection of bare ZnS substrate, which is estimated to be around 15% (R$_0 = |\frac{n-1}{n+1}|^2$, n $\approx$ 2.25, and the imaginary part is neglected). So, the extra reflection (ΔR = (γ-1)·R$_0$) due to AsP is actually a minor term (~5%) in the extinction.
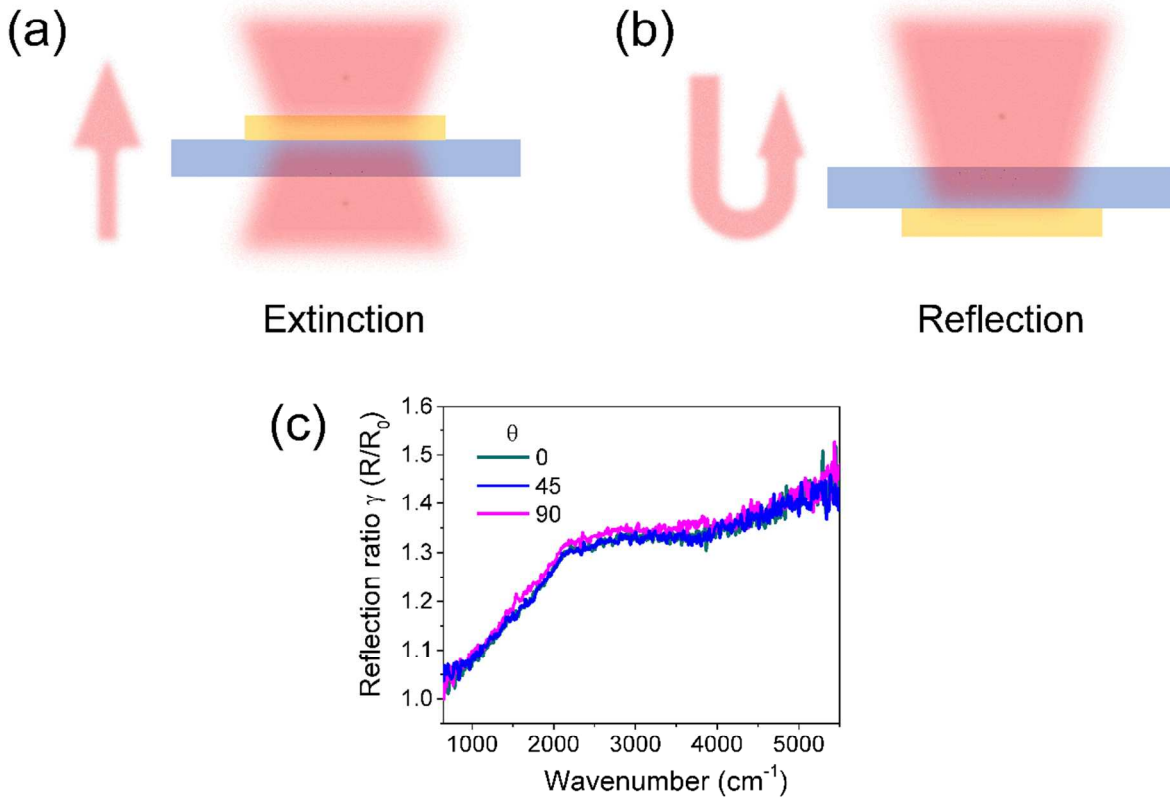

Figure S3. (a), (b) The optical configuration of infrared extinction (a) and reflection (b) measurements. **(c)** The measured infrared reflection ratio between b-As$_{0.83}$P$_{0.17}$ flake on ZnS and the bare ZnS substrate.

7

V. Calculation of noise equivalent power (NEP)

NEP is defined as the incident power, at which the signal-to-noise ratio is one in a bandwidth (Δf) of 1 Hz, $I_{ph}^2/(S_n\Delta f) = 1$, where S_n is the spectral density function of total noise.[4] NEP can be calculated as NEP $= \sqrt{S_n}/R_{ex}$. As discussed in ref. 4 in this Supporting Information, the total noise in the photoconductive devices consists of thermal noise (S_T), shot noise (S_S), and generation-recombination noise (S_{GR}), $S_n = S_T + S_S + S_{GR}$. With above consideration, we have

$$R_{ex}^2 \cdot NEP^2 = 2eI_{ds} + {4k_BT}\Big/{R} + {4eR_{ex} \cdot NEP \cdot (\tau_{life}/\tau_{tr})}\Big/{\left(1 + \left(2\pi f\tau_{life}\right)^2\right)},$$ here we set

$\Delta f = 1$ Hz. We get NEP $= \left(2e + \sqrt{4e^2\left(\frac{\tau_{life}}{\tau_{tr}}\right)^2/\left(\left(1 + \left(2\pi f\tau_{life}\right)^2\right)^2 + 2eI_{ds} + \frac{4k_BT}{R}}\right)\Big/{R_{ex}}$ by

solving the equation. We notice $4e^2\left(\frac{\tau_{life}}{\tau_{tr}}\right)^2 \ll 2eI_{ds}$ in our case, so the generation-recombination noise contributes little to the NEP in our device. For simplicity, we calculate NEP

with NEP $= \sqrt{2eI_{ds} + \frac{4k_BT}{R}}\Big/{R_{ex}}$ in the main text.

VI. Noise current density measurements at charge neutral point

Noise current density was measured with lock-in amplifier (Stanford Research SR830) and preamplifier (Femto DLPCA-200) in a Lakeshore probe station at room temperature. The tested device was biased at charge neutral point at $V_{ds} = 1$ V. The noise voltage (S_V) was acquired from lock-in amplifier and converted to noise current density by $S_I = S_V/(G \times ENBW)$, where G is the gain of the preamplifier and ENBW is the equivalent noise band-width of the lock-in amplifier. The noise measurements at each frequency were repeated twenty times consistently, and the averaged values were given in Figure S3 with error bars. Certain frequencies ($f = 60 \times n$ Hz, where n =1, 2, 3…) were intentionally avoided in the measurements to minimize the effect of 60 Hz environmental noise and its harmonics.

The measured noise current density shows clear 1/f decreasing trend from 1 to 100 Hz, while the noise current levels off above ~2 kHz. This observation indicates that the 1/f noise only dominates at very low frequencies. The measured value at high frequencies (2 to 10 kHz) is about three times as large as the calculated value, probably due to the additional noise introduced by our measurement setup.

As a result, for the intended operational speed of our detector (well above 10 kHz), it is not necessary to consider the 1/f noise.
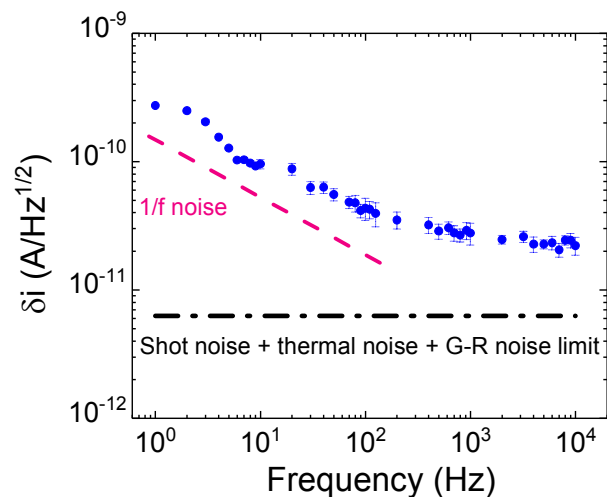
Figure S4. The measured noise current density (blue dots) at room temperature, compared with the calculated value (black dashed line). The red dashed line shows a reference 1/f noise current density.

REFERENCES

1.   Shindo, D.; Oikawa, T., *Energy Dispersive X-ray Spectroscopy*. Springer Japan: Tokyo, 2002.
2.   *Bruker SHELXTL*, V2011.4-0; Bruker AXS: Madison, WI, 2008.
3.   Muller, P.; Herbst-Irmer, R.; Spek, A.; Schneider, T.; Sawaya, M., *Crystal Structure Refinement: A Crystallographer's Guide to SHELXEL* Oxford University Press: New York, 2006.
4.   Chuang, S. L., *Physics of Photonic Devices*. John Wiley & Sons: Hoboken, 2009.